

Detecting changes in the mean of spatial random fields on a regular grid

Sheila Görz, Roland Fried

Department of Statistics, TU Dortmund University, Vogelpothsweg 87, Dortmund, 44227, North Rhine-Westphalia, Germany

Abstract

We propose statistical procedures for detecting changes in the mean of spatial random fields observed on regular grids. The proposed framework provides a general approach to change detection in spatial processes. Extending a block-based method originally developed for time series, we introduce two test statistics, one based on Gini's mean difference and a novel variance-based variant. Under mild moment conditions, we derive asymptotic normality of the variance-based statistic and prove its consistency against almost all non-constant mean functions (in a sense of positive Lebesgue measure). To accommodate spatial dependence, we further develop a de-correlation algorithm based on estimated autocovariances. Monte Carlo simulations demonstrate that both tests maintain appropriate size and power for both independent and dependent data. In an application to satellite images, especially our variance-based test reliably detects regions undergoing deforestation.

Keywords: Change region detection, Spatial random fields, Satellite images

1. Introduction

Sudden changes in the structure of data can occur not only in time series but also in spatial random fields. Applications include satellite images to detect changes in nature, medical data and quality control. In all cases, it is important that structural breaks are recognized reliably. We consider random fields (X_i) , $1 \leq i \leq n$, $n \in \mathbb{N}^d$, stemming from double arrays that follow the widely used signal-plus-noise model

$$X_i = \mu\left(\frac{i}{n}\right) + Y_i. \quad (1)$$

Here, $(Y_i)_{i \in \mathbb{N}^d}$ is a stationary random field with $E(Y_i) = 0$, $\text{Var}(Y_i) = \sigma^2$ and a continuous distribution. Our aim is to investigate whether the location function μ is constant or not. For time series, this is a well-studied problem; see e.g. Csörgő and Horváth (1997) for a survey. Many of these methods cannot be directly transferred to data over a higher-dimensional grid, as observations do not possess a natural order. Existing methods for spatial data often focus on one special type of change that should be detected. Fuentes (2005) develops a method using spatial spectral analysis where she tests if there is interaction between space and frequency through a classical ANOVA. Changes in the mean cannot be detected with this method, and it lacks asymptotic results for a growing sample size. Gromenko et al. (2017) investigate changes in the mean of observations taken at multiple spatially correlated locations. In their work, the term change refers to a change over time rather than in space. Buchchia (2014) tests for a change over a multi-dimensional "rectangle" by comparing the increase over a rectangle to the increase over the whole random field. This method needs maximization over all possible blocks and is computationally very intensive. Otto and Schmid (2016) and Kirch et al. (2025) develop methods for the detection of very specific change regions, the shape of which must be known in advance. The methods of Otto and Schmid can detect at most one change region, whereas the method of Kirch et al. (2025) can handle multiple change regions, but (asymptotic) critical values are not necessarily analytically known. Steland (2025) addresses these issues by developing a test that employs Gumbel-type extreme value theory.

Email addresses: sheila.goerz@tu-dortmund.de (Sheila Görz), msnat@statistik.tu-dortmund.de (Roland Fried)

However, the convergence of such maximum-type statistics to their asymptotical distribution can be rather slow, so that large sample sizes are needed. Another method, proposed by Zhang and Zhu (2019), focuses more on precise localization of the change region(s), but it is only applicable for independent data and abrupt changes opposed to trends. By construction, the method does not give a sensible output if no change region is present. In an application to quality control of products, Jiang et al. (2005) and Amirkhani and Amiri (2020) use ANOVA-based control charts to monitor product images. Okhrin et al. (2020) and Okhrin et al. (2025) developed methods for monitoring changes in regular grids or images while using regions of interest for dimension reduction. These methods rely on reference images and require parameters to be estimated by a pre-run. Similarly, the technique of Mayrhofer et al. (2025) requires a pre-run for outlier detection in sequences of images. All above monitoring procedures only allow for normally distributed errors and do not yield any asymptotics for growing images sizes, e.g. due to finer sampling.

Our approach is based on the work of Schmidt (2024), where blocks of a time series are compared to each other to find deviations in their location. In this study, we initially only consider the case where the Y_i from model (1) are iid. A possible non-stationarity in the mean, i.e. a change in location, is described by the function $\mu : [0, 1]^d \rightarrow \mathbb{R}$. Our work extends Schmidt's test to two-dimensional data ($d = 2$), and a transfer to higher-dimensional data is straightforward. In extending the test method, we focus on the elementary scenario of independent, homoscedastic data. However, unlike the original test statistic, we consider more options for comparing the block means.

The remainder of the paper is structured as follows. Section 2 introduces our basic assumptions and the basic test statistic. Building on this, Section 3 introduces a variance-based variation to the test statistic from Section 2, and proves its convergence and consistency against almost all non-constant mean functions. Section 4 discusses extensions to dependent data. To this end, we introduce a simple de-correlation algorithm. The results of a simulation study for both independent and dependent data are presented in Section 5, and an application to satellite data of the Amazon rainforest is given in Section 6. Section 7 provides a summary and an outlook.

2. Data situation and original test statistic

This paper focuses on the situation of 2-dimensional random fields observed on a regular grid, i.e. in our case $\mathbf{n} = (n, m)$. The data model then reads

$$X_{ij} = X_{ij}^{(n,m)} = \mu\left(\frac{i}{n}, \frac{j}{m}\right) + Y_{ij}, \quad i \in \{1, \dots, n\}, \quad j \in \{1, \dots, m\},$$

where the observations $(X_{ij}^{(n,m)})$ stem from a double array. We assume the following about the location function μ :

Assumption 1. *The location function $\mu : [0, 1]^2 \rightarrow \mathbb{R}$ is of the form: $\mu = \mu' + \sum_{i=1}^s c_i \cdot \mathbb{1}_{C_i}$ where μ' is a continuous function.*

$C_i \subset [0, 1]^2$, $i = 1, \dots, s$, are finitely many disjoint Borel sets that contain the indices over which a location shift of magnitude c_i occurs. These sets or their union $C = \bigcup_{i=1}^s C_i$ will be called "change region(s)", their complement $\mathcal{B} := [0, 1]^2 \setminus C$ will be called "base region". We assume that the boundary of each C_i has a Lebesgue measure 0 and that \mathcal{B} is not empty. Note that it is possible to have no change regions at all, even under the alternative. For example, if there is a trend present in μ , the function is continuous but not constant.

Using this notation, we want to test the hypothesis pair

$$\mathbb{H}_0 : \mu \text{ is constant} \quad \text{vs.} \quad \mathbb{H}_1 : \mu \text{ is not constant.}$$

Adapting the test statistic of Schmidt (2024) to our spatial data setting leads us to two main components.

First, the given data is divided into $b_n \times b_m$ blocks of length $l_n \times l_m$, $l_n = n_1^{s_1}$, $l_m = m_2^{s_2}$, $s_1, s_2 \in (0.5, 1)$. Then, a statistic that represents the respective block adequately is taken. The most obvious choice for this is the arithmetic mean:

$$\hat{\mu}_{hk} := \hat{\mu}_{hk}^{(n,m)} := \frac{1}{l_n l_m} \sum_{i=(h-1)l_n+1}^{hl_n} \sum_{j=(k-1)l_m+1}^{kl_m} X_{ij}, \quad h = 1, \dots, b_n, \quad k = 1, \dots, b_m.$$

A big advantage of the arithmetic mean is that its limit distribution is known and usually easy to work with. The block means form a double array

$$(\hat{\mu}_{hk}^{(n,m)}) := (\hat{\mu}_{hk}^{(n,m)}, h = 1, \dots, b_n, k = 1, \dots, b_m, n, m \in \mathbb{N})$$

since for increasing n and m , the blocks may contain different X_{ij} s. Nevertheless, the elements of the sequence $(\hat{\mu}_{hk}^{(n,m)})_{hk}$ are independent for fixed n, m .

In the second step, we apply a measure that is able to uncover possible differences between the block representatives. Schmidt (2024) uses **Gini's mean difference (GMD)**, which in our 2-dim. scenario reads as:

$$U(nm) = \frac{2}{b_n b_m (b_n b_m - 1)} \sum_{h=1}^{b_n-1} \sum_{k=1}^{b_m-1} \sum_{\substack{h'=1 \\ \neg(h=h' \wedge k=k')}}^{b_n} \sum_{k'=1}^{b_m} |\hat{\mu}_{hk} - \hat{\mu}_{h'k'}|.$$

Appropriately scaled, the following holds for the test statistic U if $\hat{\mu}$ are the arithmetic block means, the observations are independent, $E(|Y_{1,1}|^{2+\varepsilon}) < \infty$ for some $\varepsilon > 0$ and $s \in (0.5, 1)$:

$$GMD_{nm}(X) = \sqrt{b_n b_m} \left(\frac{\sqrt{l_n l_m}}{\hat{\sigma}} U(nm) - \frac{2}{\sqrt{\pi}} \right) \xrightarrow{\mathcal{D}} \mathcal{N} \left(0, \frac{4}{3} + \frac{8}{\pi} (\sqrt{3} - 2) \right)$$

with $\hat{\sigma}$ being an estimator for the standard derivation of $X_{ij}^{(n,m)}$. Both this property and the consistency of the test against almost all non-constant mean functions can be deduced from the proofs of Schmidt (2024) for the one-dimensional case. A similar test for constancy of the variance in time series was proposed by Schmidt et al. (2021).

As the arithmetic block means should asymptotically be normally distributed, regardless of the noise distribution, using the empirical variance instead of Gini's mean difference in the second step could be more efficient. Assuming the underlying data to be normally distributed, i.e. in our case $Y_{ij} \sim \mathcal{N}(0, \sigma^2)$, and that there is a fixed number of blocks $2 \leq b_{(1)}, b_{(2)} < n, m$ in each dimension, this would result in an analysis of variance (ANOVA) test to check for variability between the blocks. But since, in the classical ANOVA, the number of blocks is fixed, there are location shifts that would not be detected if the number of blocks did not increase with growing sample size respectively finer sampling. The exemplary alternative in Figure 1 demonstrates this problem graphically.

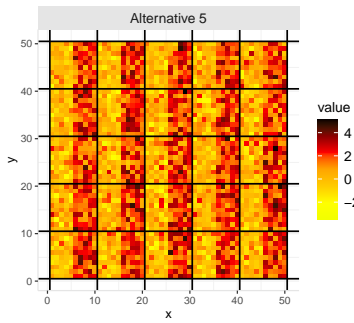


Figure 1: Example of an alternative that would not be detected if the number of blocks did not increase with growing sample size

Since, to the best of our knowledge, there are no asymptotics or modifications to cater non-normally distributed data or triangular arrays available for the ANOVA, in the next section we present a new, variance-based test statistic. We then prove its asymptotic convergence and its consistency against most alternatives.

3. A variance-based test

Instead of Gini's mean difference, we measure the variability between block means in a test based on the methods of Schmidt (2024) by their variance:

$$\frac{1}{b_n b_m} \sum_{h=1}^{b_n} \sum_{k=1}^{b_m} (\hat{\mu}_{hk} - \bar{X}_{nm})^2 = \frac{1}{b_n b_m} \sum_{h=1}^{b_n} \sum_{k=1}^{b_m} (\hat{\mu}_{hk} - \bar{\mu})^2.$$

This corresponds to the numerator of an ANOVA. In order to apply a central limit theorem (CLT), we have to scale the statistic appropriately. In the following subsections, we first introduce the final test statistic, then follows the proof of its convergence under H_0 , starting with the notation used throughout the proof. Finally, we prove the consistency of the test.

Theorem 1. *Let the assumptions (1) be fulfilled and assume that $(Y_{ij})_{1 \leq i \leq n, 1 \leq j \leq m}$ are iid and $E(|Y_{ij}|^{4+\varepsilon}) < \infty$ for all $1 \leq i \leq n, 1 \leq j \leq m$ and for some $\varepsilon > 0$. Let $\hat{\sigma}$ be a (weakly) consistent estimator for σ . Then it holds under the hypothesis of a constant mean that*

$$\frac{1}{\sqrt{2b_n b_m}} \left[\frac{l_n l_m}{\hat{\sigma}^2} \left(\sum_{h=1}^{b_n} \sum_{k=1}^{b_m} (\hat{\mu}_{hk}^{(n,m)})^2 - b_n b_m \bar{X}_{n,m}^2 \right) - b_n b_m + 1 \right] \xrightarrow{\mathcal{D}} \mathcal{N}(0, 1) \quad \text{as } N \rightarrow \infty \quad (2)$$

where $\bar{X}_{n,m} = \frac{1}{nm} \sum_{i=1}^n \sum_{j=1}^m X_{ij}$ is the arithmetic mean over all observations in the sample of size nm .

The resulting test for structural changes will be called **variance-based test** and abbreviated as **Var** in the following sections.

3.1. Notation

Define

$$\mathcal{I}_{hk} := \{(h-1)l_n + 1, \dots, hl_n\} \times \{(k-1)l_m + 1, \dots, kl_m\}, \quad h = 1, \dots, b_n; k = 1, \dots, b_m,$$

as the set of indices of observations that fall into block (h, k) . Denote with

$$\hat{v}_{hk} := \hat{v}_{hk}^{(n,m)} := \frac{1}{l_n l_m} \sum_{i,j \in \mathcal{I}_{hk}} Y_{ij} \xrightarrow{H_0} \hat{\mu}_{hk} - \mu$$

the block means of the random errors (Y_{ij}) resp. the block means $\hat{\mu}_{hk}^{(n,m)}$ if the location parameter (μ_{ij}) were constantly 0. Under H_0 , this is equal to the mean of the observations in the block minus μ . A tilde instead of a hat on an estimator indicates that the value was multiplied with the square root of the number of elements summed up, i.e. $\tilde{\mu}_{hk} = \sqrt{l_n l_m} \hat{\mu}_{hk}$ and $\tilde{v}_{hk} = \sqrt{l_n l_m} \hat{v}_{hk}$. We set $N = nm$ and use both notations interchangeably.

3.2. Motivation

In a situation with centered data with a known variance of σ^2 , the following proposition holds.

Proposition 2. *Let the assumptions (1) be fulfilled and assume that $E(|Y_{ij}|^{2+\delta}) < \infty \forall 1 \leq i \leq n, 1 \leq j \leq m$ and some $\delta > 0$. Then it holds under the hypothesis*

$$\sqrt{l_n l_m} \frac{\hat{v}_{hk}^{(n,m)}}{\sigma} \xrightarrow{\mathcal{D}} \mathcal{N}(0, 1) \quad \forall 1 \leq h \leq b_n, 1 \leq k \leq b_m.$$

This convergence holds according to the central limit theorem for double arrays, see Serfling (1980, p. 31-32). A more detailed proof is given in the appendix.

Remark 3. *According to the Continuous Mapping Theorem,*

$$l_n l_m \frac{\hat{v}_{hk}^2}{\sigma^2} \xrightarrow{\mathcal{D}} \mathcal{N}(0, 1)^2 = \chi_1^2 \quad \text{and} \quad \frac{l_n l_m}{\sigma^2} \sum_{h=1}^a \sum_{k=1}^b \hat{v}_{hk}^2 \xrightarrow{\mathcal{D}} \chi_{ab}^2$$

for any $a \in \{1, \dots, b_n\}$ and $b \in \{1, \dots, b_m\}$.

3.3. Proof of Theorem 1

In practice, we cannot assume (μ_{ij}) to be constantly equal to 0 and we need to center the block means to derive a sensible CLT. Consider therefore the block means centered by the overall arithmetic mean:

$$\begin{aligned}
\sqrt{l_n l_m} (\hat{\mu}_{hk}^{(n,m)} - \bar{X}) &= \sqrt{l_n l_m} \left[\frac{1}{l_n l_m} \sum_{i,j \in \mathcal{I}_{hk}} X_{ij} - \bar{X} \right] \\
&= \sqrt{l_n l_m} \left[\frac{1}{l_n l_m} \sum_{i,j \in \mathcal{I}_{hk}} (\mu + Y_{ij}) - (\mu + \bar{Y}) \right] \\
&= \sqrt{l_n l_m} \left[\frac{1}{l_n l_m} \sum_{i,j \in \mathcal{I}_{hk}} Y_{ij} - \bar{Y} \right] \\
&= \sqrt{l_n l_m} (\hat{v}_{hk}^{(n,m)} - \bar{Y}) \\
&= \tilde{v}_{hk}^{(n,m)} - \sqrt{l_n l_m} \bar{Y}, \quad h = 1, \dots, b_n, k = 1, \dots, b_m.
\end{aligned}$$

Analogously, for the weighted sum of the squared values we can write

$$\begin{aligned}
\frac{l_n l_m}{\sqrt{b_n b_m}} \sum_{h=1}^{b_n} \sum_{k=1}^{b_m} (\hat{\mu}_{hk} - \bar{X})^2 &= \frac{l_n l_m}{\sqrt{b_n b_m}} \sum_{h=1}^{b_n} \sum_{k=1}^{b_m} (\hat{v}_{hk} - \bar{Y})^2 \\
&= \frac{l_n l_m}{\sqrt{b_n b_m}} \left[\sum_{h=1}^{b_n} \sum_{k=1}^{b_m} \hat{v}_{hk}^2 - b_n b_m \bar{Y}^2 \right] \\
&= \frac{1}{\sqrt{b_n b_m}} \left[\sum_{h=1}^{b_n} \sum_{k=1}^{b_m} \tilde{v}_{hk}^2 - nm \bar{Y}^2 \right]
\end{aligned}$$

since $\bar{Y} = \frac{1}{b_n b_m} \sum_{h=1}^{b_n} \sum_{k=1}^{b_m} \hat{v}_{hk}$. For the overall mean, it holds $E(\bar{Y}^2) = \frac{\sigma^2}{nm}$.

We can rewrite term (2) in Theorem 1 as

$$(2) = \frac{1}{\sqrt{2}} \left(\frac{l_n l_m}{\hat{\sigma}^2 \sqrt{b_n b_m}} \sum_{h=1}^{b_n} \sum_{k=1}^{b_m} \tilde{v}_{hk}^2 - \sqrt{b_n b_m} \right) \quad (3)$$

$$- \frac{1}{\sqrt{2}} \left(\frac{l_n l_m \sqrt{b_n b_m}}{\hat{\sigma}^2} \bar{Y}^2 - \frac{1}{\sqrt{b_n b_m}} \right). \quad (4)$$

The first term of the above difference contains the variance estimation on the block means and we can show that the Central Limit Theorem holds. The second term contains the centering by the arithmetic mean and we will show that it is asymptotically negligible. Before that, we introduce the following lemma which we will use later.

Lemma 4. Let $(Y_{ij})_{\substack{1 \leq i \leq n \\ 1 \leq j \leq m}}$ be i.i.d. random variables with $E(Y_{1,1}) = 0$, $Var(Y_{1,1}) = \sigma^2$ and $E(|Y_{1,1}|^{4+\delta}) < \infty$ for $\delta > 0$. Denote with $\kappa_{n,m}^{(4)}$ the fourth standardized moment of the distribution of $\frac{1}{\sqrt{nm}} \sum_{i=1}^n \sum_{j=1}^m Y_{ij}$. Then

$$\kappa_{n,m}^{(4)} = E \left[\frac{\left(\sum_{i=1}^n \sum_{j=1}^m Y_{ij} \right)^4}{N^2 \sigma^4} \right] = E \left[\frac{N^2 \bar{Y}_{n,m}^4}{\sigma^4} \right] \rightarrow 3 \quad \text{as } N \rightarrow \infty.$$

Proof. First, we notice that according to Proposition 2, $\frac{\sqrt{nm} \bar{Y}_{n,m}}{\sigma} \xrightarrow{\mathcal{D}} \mathcal{N}(0, 1)$ and with the Continuous Mapping Theorem, $\left[\frac{\sqrt{nm} \bar{Y}_{n,m}}{\sigma} \right]^4 \xrightarrow{\mathcal{D}} \mathcal{N}(0, 1)^4$.

Next we show that $\left\{ \frac{N^2 \tilde{Y}_{n,m}^4}{\sigma^4} \mid n \geq 1, m \geq 1 \right\}$ is uniformly integrable. For n and m large enough we can apply Theorem 2 from Brillinger (1962) and get

$$E \left[\left(\frac{\left(\sum_{i=1}^n \sum_{j=1}^m Y_{ij} \right)^4}{N^2 \sigma^4} \right)^{1+\delta} \right] < C < \infty,$$

for a positive constant C . For smaller n and m , the inequality trivially holds. According to the postscript to Theorem 5.3 in Billingsley (2013, p. 32), $\left\{ \frac{N^2 \tilde{Y}_{n,m}^4}{\sigma^4} \mid n \geq 1, m \geq 1 \right\}$ is therefore uniformly integrable. We can apply Theorem 5.4 from Billingsley (2013, p. 32) and conclude that

$$\kappa_{n,m}^{(4)} = E \left[\frac{N^2 \tilde{Y}_{n,m}^4}{\sigma^4} \right] \rightarrow E(Z^4), \quad Z \sim \mathcal{N}(0, 1).$$

The fourth moment of a standard normal distribution is known to be 3. \square

Theorem 5. *Let the assumptions (1) be fulfilled and assume that $E(|Y_{ij}|^{4+\varepsilon}) < \infty \forall 1 \leq i \leq n, 1 \leq j \leq m$ and for $\varepsilon > 0$. Then it holds under the hypothesis*

$$\frac{1}{\sqrt{\kappa_{l_n, l_m}^{(4)} - 1}} \left[\frac{1}{\sigma^2 \sqrt{b_n b_m}} \sum_{h=1}^{b_n} \sum_{k=1}^{b_m} (\tilde{v}_{hk}^{(n,m)})^2 - \sqrt{b_n b_m} \right] \xrightarrow{\mathcal{D}} \mathcal{N}(0, 1) \text{ as } N \rightarrow \infty$$

Proof.

$$(\hat{v}_{hk}^{(n,m)}) = (\hat{v}_{hk}^{(n,m)}, h = 1, \dots, b_n, k = 1, \dots, b_m, n, m \in \mathbb{N})$$

is a double array, so $(\hat{v}_{hk}^{(n,m)})^2$ is one, too. We notice that since the Y_{ij} s are independent, the weighted, centered and squared non-overlapping block means (\tilde{v}_{hk}^2) are independent as well. Following from the independence, we get that

$$E(l_n l_m \hat{v}_{hk}^2) = E(\tilde{v}_{hk}^2) = \text{Var}(\tilde{v}_{hk}) + \underbrace{E(\tilde{v}_{hk})^2}_{=0} = \frac{1}{l_n l_m} \sum_{i,j \in \mathcal{I}_{hk}} \text{Var}(Y_{ij}) = \sigma^2$$

and

$$\text{Var}(l_n l_m \hat{v}_{hk}^2) = E(\tilde{v}_{hk}^4) - E(\tilde{v}_{hk}^2)^2 = E \left(\left(\frac{1}{\sqrt{l_n l_m}} \sum_{i,j \in \mathcal{I}_{hk}} Y_{ij} \right)^4 \right) - \sigma^4 = \sigma^4 (\kappa_{l_n, l_m}^{(4)} - 1)$$

where $\kappa_{l_n, l_m}^{(4)}$ is the fourth standardized moment of the distribution of \tilde{v}_{hk}^4 . By using Theorem 2 from Brillinger (1962), we can show that the variance given in the last equation is indeed finite. According to Brillinger (1962),

$$\text{Var}(\tilde{v}_{hk}^2) = \sigma^4 (\kappa_{l_n, l_m}^{(4)} - 1) = \frac{1}{(l_n l_m)^2} E \left[\left(\sum_{i,j \in \mathcal{I}_{hk}} Y_{ij} \right)^4 \right] - \sigma^4 < C - \sigma^4 < \infty$$

for all h, k , for a $C > 0$ and n, m large enough as long as the Y_{ij} are i.i.d. and $E(|Y_{1,1}|^4) < \infty$, as assumed.

A detailed verification of Lyapunov's condition is given in the appendix. According to the CLT for triangular arrays, Theorem 5 holds. \square

Verification of Lyapunov's condition. Choosing $\delta = \varepsilon/2$, we need to verify that

$$\lim_{n \rightarrow \infty} \frac{1}{\left(\sum_{h=1}^{b_n} \sum_{k=1}^{b_m} \text{Var}(\tilde{v}_{hk}^2) \right)^{1+\frac{\delta}{2}}} \sum_{h=1}^{b_n} \sum_{k=1}^{b_m} E \left[|\tilde{v}_{hk}^2 - \sigma^2|^{2+\delta} \right] = 0.$$

Since $\tilde{\mu}_{hk}^2$ and σ^2 are both positive (first step), by the c_r -inequality (second step), and by using again Theorem 2 from Brillinger (1962) (fourth step), we get for the numerator

$$\begin{aligned} \sum_{h=1}^{b_n} \sum_{k=1}^{b_m} \mathbb{E} \left[|\tilde{\nu}_{hk}^2 - \sigma^2|^{2+\delta} \right] &\leq \sum_{h=1}^{b_n} \sum_{k=1}^{b_m} \mathbb{E} \left[|\tilde{\nu}_{hk}^2 + \sigma^2|^{2+\delta} \right] \\ &\leq \text{const} \cdot \sum_{h=1}^{b_n} \sum_{k=1}^{b_m} \left(\mathbb{E} (|\tilde{\nu}_{hk}|^{4+\varepsilon}) + \sigma^{4+\varepsilon} \right) \\ &= \text{const} \cdot \sum_{h=1}^{b_n} \sum_{k=1}^{b_m} \left(\frac{1}{(l_n l_m)^{2+\delta}} \mathbb{E} \left(\left| \sum_{i,j \in T_{hk}} Y_{ij} \right|^{4+\varepsilon} \right) + \sigma^{4+\varepsilon} \right) \\ &< \text{const} \cdot b_n b_m \end{aligned}$$

for n, m large enough and $\mathbb{E}(|Y_{1,1}|^{4+\varepsilon}) < \infty$, as assumed. Now considering the denominator, we have

$$\sum_{h=1}^{b_n} \sum_{k=1}^{b_m} \text{Var}(\tilde{\nu}_{hk}^2) = b_n b_m \cdot \sigma^4 (\kappa_{l_n, l_m}^{(4)} - 1),$$

so in total, we get

$$\frac{1}{\left(\sum_{h=1}^{b_n} \sum_{k=1}^{b_m} \text{Var}(\tilde{\nu}_{hk}^2) \right)^{1+\frac{\delta}{2}}} \sum_{h=1}^{b_n} \sum_{k=1}^{b_m} \mathbb{E} \left[|\tilde{\nu}_{hk}^2 - \sigma^2|^{2+\delta} \right] < \frac{\text{const}}{(b_n b_m)^{\frac{\delta}{2}}} \underbrace{(\kappa_{l_n, l_m}^{(4)} - 1)}_{\rightarrow 2}^{-(1+\frac{\delta}{2})} = O\left(\frac{1}{(b_n b_m)^{\frac{\delta}{2}}}\right).$$

□

As the following proposition shows, the terms $\kappa_{l_n, l_m}^{(4)}$ and σ^2 in Theorem 5 can be replaced by the corresponding limit value resp. estimator.

Proposition 6. *Let the assumptions (1) be fulfilled and let $\hat{\sigma}^2$ be a consistent estimator for σ^2 that converges in $O\left(\frac{1}{\sqrt{N}}\right)$. Then it holds under the hypothesis*

$$\frac{1}{\sqrt{2}} \left(\frac{l_n l_m}{\hat{\sigma}^2 \sqrt{b_n b_m}} \sum_{h=1}^{b_n} \sum_{k=1}^{b_m} \hat{\nu}_{hk}^2 - \sqrt{b_n b_m} \right) \xrightarrow{\mathcal{D}} \mathcal{N}(0, 1)$$

Proof.

$$\begin{aligned} &\frac{1}{\sqrt{2}} \left(\frac{l_n l_m}{\hat{\sigma}^2 \sqrt{b_n b_m}} \sum_{h=1}^{b_n} \sum_{k=1}^{b_m} \hat{\nu}_{hk}^2 - \sqrt{b_n b_m} \right) \\ &= \underbrace{\frac{1}{\sqrt{\kappa_{l_n, l_m}^{(4)} - 1}} \left(\frac{l_n l_m}{\sigma^2 \sqrt{b_n b_m}} \sum_{h=1}^{b_n} \sum_{k=1}^{b_m} \hat{\nu}_{hk}^2 - \sqrt{b_n b_m} \right)}_{\xrightarrow{\mathcal{D}} \mathcal{N}(0, 1) \text{ according to Theorem 5}} \frac{\sigma^2}{\hat{\sigma}^2} \sqrt{\frac{\kappa_{l_n, l_m}^{(4)} - 1}{2}} + \sqrt{\frac{b_n b_m}{2}} \left(\frac{\sigma^2}{\hat{\sigma}^2} - 1 \right) \end{aligned}$$

$\frac{\hat{\sigma}^2}{\sigma^2} \rightarrow 1$ since $\hat{\sigma}^2$ is a consistent estimator for σ^2 and as per the CMT, $\frac{\sigma^2}{\hat{\sigma}^2} \rightarrow 1$, too. $\sqrt{\frac{\kappa_{l_n, l_m}^{(4)} - 1}{2}} \rightarrow \sqrt{\frac{2}{2}} = 1$ holds according to Lemma 4. Therefore, by application of Slutsky's lemma, we get the convergence in distribution of the first summand to a standard normal distribution.

For the second summand, we know that $\sigma^2 - \hat{\sigma}^2$ converges to 0 in $O\left(\frac{1}{\sqrt{N}}\right)$, hence

$$\sqrt{\frac{b_n b_m}{2}} \frac{\sigma^2 - \hat{\sigma}^2}{\sigma^2} = \sqrt{\frac{N^{1-s}}{2}} \frac{\sigma^2 - \hat{\sigma}^2}{\sigma^2} \rightarrow 0 \quad (N \rightarrow \infty)$$

as long as $s < 1$. And with the same argument as before,

$$\sqrt{\frac{b_n b_m}{2}} \frac{\sigma^2 - \hat{\sigma}^2}{\sigma^2} \frac{\sigma^2}{\hat{\sigma}^2} = \sqrt{\frac{b_n b_m}{2}} \left(\frac{\sigma^2}{\hat{\sigma}^2} - 1 \right) \rightarrow 0 \quad (N \rightarrow \infty).$$

Another application of Slutsky's lemma proves the proposition. \square

Remark 7. The empirical variance $\frac{1}{n-1} \sum_{i=1}^n \sum_{j=1}^m (X_{ij} - \bar{X})^2$ over all observations of the random field is a consistent estimator for σ^2 under H_0 . As long as $E(|Y|^4) < \infty$, which is assumed throughout this paper, the empirical variance converges to σ^2 in $O(\frac{1}{N})$ (Serfling (1980), p. 192).

Proposition 8. Let $\hat{\sigma}^2$ be a (weakly) consistent estimator for σ^2 . Then

$$\frac{1}{\sqrt{2}} \left(\frac{l_n l_m \sqrt{b_n b_m}}{\hat{\sigma}^2} \bar{Y}^2 - \frac{1}{\sqrt{b_n b_m}} \right) \xrightarrow{P} 0 \quad \text{as } n, m \rightarrow \infty.$$

Proof. Application of Markov's inequality yields

$$\begin{aligned} P \left(\left| \frac{1}{\sqrt{2}} \left(\frac{l_n l_m \sqrt{b_n b_m}}{\hat{\sigma}^2} \bar{Y}^2 - \frac{1}{\sqrt{b_n b_m}} \right) \right| > \varepsilon \right) &\leq \frac{1}{\varepsilon} E \left(\left| \frac{1}{\sqrt{2}} \left(\frac{l_n l_m \sqrt{b_n b_m}}{\hat{\sigma}^2} \bar{Y}^2 - \frac{1}{\sqrt{b_n b_m}} \right) \right| \right) \\ &\leq \frac{l_n l_m \sqrt{b_n b_m}}{\varepsilon \sqrt{2} \hat{\sigma}^2} E(\bar{Y}^2) + \frac{1}{\varepsilon \sqrt{b_n b_m}} = \frac{l_n l_m \sqrt{b_n b_m} \sigma^2}{\varepsilon \sqrt{2} \hat{\sigma}^2 n m} + \frac{1}{\varepsilon \sqrt{b_n b_m}} \\ &= \frac{1}{\varepsilon \sqrt{2 b_n b_m}} \underbrace{\frac{\sigma^2}{\hat{\sigma}^2}}_{\rightarrow 1} + \frac{1}{\varepsilon \sqrt{b_n b_m}} \\ &\rightarrow 0 \quad (n, m \rightarrow \infty). \end{aligned}$$

\square

Rewriting term (2) in Theorem 1 leads us to

$$(2) = \frac{1}{\sqrt{2}} \left(\frac{l_n l_m}{\hat{\sigma}^2 \sqrt{b_n b_m}} \sum_{h=1}^{b_n} \sum_{k=1}^{b_m} \hat{\nu}_{hk}^2 - \sqrt{b_n b_m} \right) - \frac{1}{\sqrt{2}} \left(\frac{l_n l_m \sqrt{b_n b_m}}{\sigma^2} \bar{Y}^2 - \frac{1}{\sqrt{b_n b_m}} \right)$$

The convergence of the first term of the difference to a standard normal distribution holds with a combination of Theorem 5, Lemma 4 and Slutsky's lemma. With Proposition 8 and a second application of Slutsky's lemma, Theorem 1 is proven.

Remark 9. Note that we included a "+1" in (2) as a counteraction of the effect of \bar{X}^2 on the mean of the entire test statistic. This is negligible for the asymptotic result. However, since b_n and b_m tend to be rather small even in moderate sample sizes, simulations have shown that its inclusion is beneficial to the power of the test.

3.4. Consistency under the Alternative

Theorem 10. Let the assumptions (1) be fulfilled. Then both under the hypothesis and the alternative it holds that

$$T(n, m) := \frac{1}{b_n b_m} \sum_{h=1}^{b_n} \sum_{k=1}^{b_m} (\hat{\mu}_{hk} - \bar{X})^2 \xrightarrow{L^2} \int_0^1 \int_0^1 \left(\mu(x, y) - \int_0^1 \int_0^1 \mu(u, v) du dv \right)^2 dx dy \quad \text{as } n, m \rightarrow \infty.$$

The double integral above determines the variability of the function μ . It is well known that it is 0 if and only if μ is constant except for Lebesgue-negligible sets. Due to this, it follows that the test is consistent against all other non-constant mean functions.

Proof. In this proof, we use the shortening notation $\mu_{x,y} := \mu\left(\frac{x}{b_n}, \frac{y}{b_m}\right)$. Denote with $\mu_{sup} := \sup_{x,y \in [0,1]} |\mu(x,y)|$ the maximal absolute value μ takes.

First, we show that

$$T(n,m) \approx \frac{1}{b_n b_m} \sum_{h=1}^{b_n} \sum_{k=1}^{b_m} (\mu_{hl_n,kl_m} - \bar{\mu}_{l_n,l_m})^2,$$

i.e. the arguments in the variance function in T can be replaced by deterministic ones. The $\mu_{hl_n,kl_m} = \mu\left(\frac{h}{b_n}, \frac{k}{b_m}\right)$ can be seen as "block representatives" opposed to the block means $\hat{\mu}_{hk}$ in the original function T . Then $\bar{\mu}_{l_n,l_m} := \frac{1}{b_n b_m} \sum_{h=1}^{b_n} \sum_{k=1}^{b_m} \mu_{hl_n,kl_m}$ is the mean over all block representatives. Since $X_{ij} = \mu_{i,j} + Y_{ij}$ it follows that

$$\hat{\mu}_{hk} = \frac{1}{l_n l_m} \sum_{i,j \in I_{hk}} X_{ij} = \frac{1}{l_n l_m} \sum_{i,j \in I_{hk}} (\mu_{i,j} + Y_{ij}) = \bar{\mu}_{hk} + \bar{Y}_{hk}.$$

Using this, $T(n,m)$ can be written as

$$\begin{aligned} T(n,m) &= \frac{1}{b_n b_m} \sum_{h=1}^{b_n} \sum_{k=1}^{b_m} (\hat{\mu}_{hk} - \bar{X})^2 \\ &= \frac{1}{b_n b_m} \sum_{h=1}^{b_n} \sum_{k=1}^{b_m} \left(\frac{1}{l_n l_m} \sum_{i=(h-1)l_n+1}^{hl_n} (\mu_{i,j} + Y_{ij}) - \frac{1}{n} \sum_{i=1}^n \sum_{j=1}^m (\mu_{i,j} + Y_{ij}) \right)^2 \\ &= \frac{1}{b_n b_m} \sum_{h=1}^{b_n} \sum_{k=1}^{b_m} (\bar{\mu}_{hk} - \bar{\mu} + \bar{Y}_{hk} - \bar{Y})^2 \\ &= \frac{1}{b_n b_m} \sum_{h=1}^{b_n} \sum_{k=1}^{b_m} ((\bar{\mu}_{hk} - \bar{\mu})^2 + 2(\bar{\mu}_{hk} - \bar{\mu})(\bar{Y}_{hk} - \bar{Y}) + (\bar{Y}_{hk} - \bar{Y})^2). \end{aligned}$$

Consequently,

$$\begin{aligned} &\left| T(n,m) - \frac{1}{b_n b_m} \sum_{h=1}^{b_n} \sum_{k=1}^{b_m} (\mu_{hl_n,kl_m} - \bar{\mu}_{l_n,l_m})^2 \right| \\ &= \left| \frac{1}{b_n b_m} \sum_{h=1}^{b_n} \sum_{k=1}^{b_m} ((\bar{\mu}_{hk} - \bar{\mu})^2 - (\mu_{hl_n,kl_m} - \bar{\mu}_{l_n,l_m})^2 + 2(\bar{\mu}_{hk} - \bar{\mu})(\bar{Y}_{hk} - \bar{Y}) + (\bar{Y}_{hk} - \bar{Y})^2) \right| \\ &\leq \underbrace{\left| \frac{1}{b_n b_m} \sum_{h=1}^{b_n} \sum_{k=1}^{b_m} ((\bar{\mu}_{hk} - \bar{\mu})^2 - (\mu_{hl_n,kl_m} - \bar{\mu}_{l_n,l_m})^2) \right|}_{(I)} + \underbrace{\left| \frac{1}{b_n b_m} \sum_{h=1}^{b_n} \sum_{k=1}^{b_m} (\bar{Y}_{hk} - \bar{Y})^2 \right|}_{(II)} \\ &\quad + \underbrace{\left| \frac{2}{b_n b_m} \sum_{h=1}^{b_n} \sum_{k=1}^{b_m} (\bar{\mu}_{hk} - \bar{\mu})(\bar{Y}_{hk} - \bar{Y}) \right|}_{(III)}. \end{aligned}$$

We will now treat each of the three terms individually.

(I): Turning to the first part of the term, we have to make sure to include possible change regions C_1, \dots, C_r into the calculation. As long as Assumption (1) holds, we can divide the blocks into two sets. Denote with $\mathcal{R}^{(1)}$ the set of indices $1 \leq h \leq b_n, 1 \leq k \leq b_m$ where the block with index (h,k) intersects with exactly one region (either with or without change). Accordingly, $\mathcal{R}^{(+)}$ is the set of those indices where the corresponding blocks intersect with more than one region. There is only a finite number $s^{(n,m)} \leq b_n \cdot b_m$ of blocks that intersect with more than one region. Consider a function $h_{n,m} : [0,1]^2 \rightarrow \{0,1\}$,

$$h_{n,m}(x,y) := \begin{cases} 1, & \text{if } (x,y) \in \mathcal{I}_{hk} \text{ with } \mathcal{I}_{hk} \cap \mathcal{R}^{(+)} \neq \emptyset \\ 0, & \text{else} \end{cases}$$

that indicates whether a pair of indices (x, y) lies in a block that intersects with more than one region or not. Then

$$\int_0^1 \int_0^1 h_{n,m}(x, y) dx dy = s^{(n,m)} \frac{l_n l_m}{N} = \frac{s^{(n,m)}}{b_n b_m}$$

corresponds to a Darboux (Riemann) upper sum of the Riemann integral over the boundaries between two regions.

Since we assume that the Lebesgue measure over the boundaries exist and is 0, we get that $\frac{s^{(n,m)}}{b_n b_m} \xrightarrow{N} 0$.

Now term (I) can be split up as follows:

$$\begin{aligned} \left| \frac{1}{b_n b_m} \sum_{h=1}^{b_n} \sum_{k=1}^{b_m} \left((\bar{\mu}_{hk} - \bar{\mu})^2 - (\mu_{hl_n, kl_m} - \bar{\mu}_{l_n, l_m})^2 \right) \right| &= \left| \frac{1}{b_n b_m} \sum_{h=1}^{b_n} \sum_{k=1}^{b_m} \left((\bar{\mu}_{hk}^2 - \bar{\mu}^2) - (\mu_{hl_n, kl_m}^2 - \bar{\mu}_{l_n, l_m}^2) \right) \right| \\ &= \left| \frac{1}{b_n b_m} \sum_{h=1}^{b_n} \sum_{k=1}^{b_m} \left(\bar{\mu}_{hk}^2 - \mu_{hl_n, kl_m}^2 - \bar{\mu}^2 + \bar{\mu}_{l_n, l_m}^2 \right) \right| \\ &\leq \frac{1}{b_n b_m} \sum_{h=1}^{b_n} \sum_{k=1}^{b_m} \left| \bar{\mu}_{hk}^2 - \mu_{hl_n, kl_m}^2 \right| + \left| \bar{\mu}^2 - \bar{\mu}_{l_n, l_m}^2 \right| \end{aligned}$$

To find an upper bound, we can make use of the continuity of the function μ over $\mathcal{R}^{(1)}$. For some arbitrary $(i, j) \in \mathcal{I}_{hk}$ it follows

$$d\left(\left(\frac{i}{n}, \frac{j}{m}\right), \left(\frac{h}{b_n}, \frac{k}{b_m}\right)\right) \leq d\left(\left(\frac{(h-1)l_n + 1}{n}, \frac{(k-1)l_m + 1}{m}\right), \left(\frac{h}{b_n}, \frac{k}{b_m}\right)\right) \rightarrow 0$$

since both $\left| \frac{(h-1)l_n + 1}{n} - \frac{h}{b_n} \right| \rightarrow 0$ and $\left| \frac{(k-1)l_m + 1}{m} - \frac{k}{b_m} \right| \rightarrow 0$ $\forall h, k$ as $n, m \rightarrow \infty$. As μ' is continuous and therefore uniformly continuous over $[0, 1]$, it holds that $\forall \delta > 0 \exists \tilde{n}, \tilde{m} \in \mathbb{N}$ such that

$$\max_{(h,k) \in \mathcal{R}^{(1)}} \sup_{(i,j) \in \mathcal{I}_{hk}} |\mu_{ij} - \mu_{hl_n, kl_m}| = |\mu'_{ij} - \mu'_{hl_n, kl_m}| < \delta \quad \forall n > \tilde{n}, m > \tilde{m}.$$

This inequality still applies if we replace μ_{ij} with the corresponding arithmetic block mean $\bar{\mu}_{hk}$. From the uniform continuity of the function $g : x \mapsto x^2$ over $[0, 1]^2$ it follows that $\forall \varepsilon_1 > 0 \exists \tilde{n}, \tilde{m} \in \mathbb{N}$ with

$$\max_{(h,k) \in \mathcal{R}^{(1)}} |\bar{\mu}_{hk}^2 - \mu_{hl_n, kl_m}^2| < \varepsilon_1 \quad \forall n > \tilde{n}, m > \tilde{m}.$$

On the other hand, for all $(h, k) \in \mathcal{R}^{(+)}$ we get $|\bar{\mu}_{hk}^2 - \mu_{hl_n, kl_m}^2| \leq 2\mu_{sup}^2$. Consequently,

$$\frac{1}{b_n b_m} \sum_{h=1}^{b_n} \sum_{k=1}^{b_m} |\bar{\mu}_{hk}^2 - \mu_{hl_n, kl_m}^2| < \frac{2s}{b_n b_m} \mu_{sup}^2 + \frac{b_n b_m - s}{b_n b_m} \varepsilon_1 < \varepsilon_1 \quad (5)$$

for n, m large enough.

Turning to the second term, for all $(h, k) \in \mathcal{R}^{(1)}$ we have $|\bar{\mu}_{hk} - \mu_{hl_n, kl_m}| < \delta$ for n, m sufficiently large as above. For $(h, k) \in \mathcal{R}^{(+)}$ we get that $|\bar{\mu}_{hk} - \mu_{hl_n, kl_m}| \leq 2\mu_{sup}$. In total, this yields

$$|\bar{\mu} - \bar{\mu}_{l_n, l_m}| \leq \frac{1}{b_n b_m} \sum_{h=1}^{b_n} \sum_{k=1}^{b_m} |\bar{\mu}_{hk} - \mu_{hl_n, kl_m}| < \frac{2s}{b_n b_m} \mu_{sup} + \frac{b_n b_m - s}{b_n b_m} \delta < \delta$$

for n, m large enough and by continuity we derive that $\forall \varepsilon_2 > 0 \exists \tilde{n}, \tilde{m} \in \mathbb{N}$ such that

$$|\bar{\mu}^2 - \bar{\mu}_{l_n, l_m}^2| < \varepsilon_2 \quad \forall n > \tilde{n}, m > \tilde{m}. \quad (6)$$

Combining (5) and (6), we get

$$\frac{1}{b_n b_m} \sum_{h=1}^{b_n} \sum_{k=1}^{b_m} |\bar{\mu}_{hk}^2 - \mu_{hl_n, kl_m}^2| + |\bar{\mu}^2 - \bar{\mu}_{l_n, l_m}^2| < \varepsilon_1 + \varepsilon_2 < \varepsilon$$

for nm large enough.

(II): $\frac{1}{b_n b_m} \sum_{h=1}^{b_n} \sum_{k=1}^{b_m} (\bar{Y}_{hk} - \bar{Y})^2$ is a (weakly) consistent estimator for the variance of the mean over all Y_{ij} in one block since the Y_{ij} are iid, and so are the block-wise means. From this, it follows

$$\begin{aligned} \frac{l_n l_m}{b_n b_m} \sum_{h=1}^{b_n} \sum_{k=1}^{b_m} (\bar{Y}_{hk} - \bar{Y})^2 &= \frac{1}{b_n b_m} \sum_{h=1}^{b_n} \sum_{k=1}^{b_m} (\sqrt{l_n l_m} \bar{Y}_{hk} - \sqrt{l_n l_m} \bar{Y})^2 = \widehat{\text{Var}}(\bar{Y}_{1,1}) \\ &\rightarrow l_n l_m \frac{\sigma^2}{l_n l_m} = \sigma^2. \end{aligned}$$

Thus, $\frac{1}{b_n b_m} \sum_{h=1}^{b_n} \sum_{k=1}^{b_m} (\bar{Y}_{hk} - \bar{Y})^2 \rightarrow 0$ in probability.

(III): Using the Cauchy-Schwarz-inequality, we get

$$\left| \frac{2}{b_n b_m} \sum_{h=1}^{b_n} \sum_{k=1}^{b_m} (\bar{\mu}_{hk} - \bar{\mu})(\bar{Y}_{hk} - \bar{Y}) \right| \leq \sqrt{\frac{2}{b_n b_m} \sum_{h=1}^{b_n} \sum_{k=1}^{b_m} (\bar{\mu}_{hk} - \bar{\mu})^2} \cdot \sqrt{\frac{2}{b_n b_m} \sum_{h=1}^{b_n} \sum_{k=1}^{b_m} (\bar{Y}_{hk} - \bar{Y})^2}.$$

The first term is bounded since

$$\sqrt{\frac{2}{b_n b_m} \sum_{h=1}^{b_n} \sum_{k=1}^{b_m} (\bar{\mu}_{hk} - \bar{\mu})^2} \leq \sqrt{2} (\max(\mu) - \min(\mu)) = \text{const.}$$

Analogously to (II), for the second term we get that

$$\sqrt{\frac{2}{b_n b_m} \sum_{h=1}^{b_n} \sum_{k=1}^{b_m} (\bar{Y}_{hk} - \bar{Y})^2} \xrightarrow{nm \rightarrow \infty} 0 \text{ in probability.}$$

In total, we get that the term (III) converges to 0 as nm goes to ∞ .

It remains to show that

$$\frac{1}{b_n b_m} \sum_{h=1}^{b_n} \sum_{k=1}^{b_m} (\mu_{h l_n, k l_m} - \bar{\mu}_{l_n, l_m})^2 \rightarrow \int_0^1 \int_0^1 \left(\mu(x, y) - \int_0^1 \int_0^1 \mu(u, v) dudv \right)^2 dxdy.$$

By construction, the discontinuities of the location function μ form a Lebesgue null set and μ is bounded on $[0, 1]^2$. Hence

$$\bar{\mu}_{l_n, l_m} = \frac{1}{b_n b_m} \sum_{h=1}^{b_n} \sum_{k=1}^{b_m} \mu_{h l_n, k l_m} \rightarrow \int_0^1 \int_0^1 \mu(u, v) dudv$$

by Lebesgue's integrability criterion for multiple Riemann integrals (e.g. Theorem 14.5 in Apostol (1974)). Similarly, for an arbitrary constant $C \in \mathbb{R}$, $g_C(x, y) := (\mu(x, y) - C)^2$ has only discontinuities with Lebesgue-measure 0 and is bounded on $[0, 1]^2$. By Lebesgue's integrability criterion for multiple Riemann integrals, and by choosing $C = \int_0^1 \int_0^1 \mu(x, y) dxdy$, we get the desired convergence. \square

4. De-correlation

One option to make the tests applicable to dependent data is to remove the correlation in the data beforehand. This can either be done by fitting a suitable model and working with the residuals, or, if the structure of the data is unknown or no suitable model exists, one can de-correlate the data using their sample autocovariance. This is a well-established procedure, proposed e.g. by Robbins et al. (2011) for detecting a shift in time series. According to

their study, tests especially designed for dependent data only have a slightly higher power than tests for independent data applied to one-step-ahead predictions, but they come with substantial computational complexities. Other reasons to avoid tests adapted to dependence may be analytically unknown critical values or strict model assumptions that prevent the adapted test to be generalized to broader settings.

The basis for our de-correlation algorithm is the assumption of stationarity of the data. We then need to estimate their autocovariances $\gamma(\mathbf{h})$ for all relevant lags $\mathbf{h} = (h_1, h_2)$. This is done by the empirical estimator

$$\hat{\gamma}_{\text{reg}}(h_1, h_2) = \frac{1}{N} \sum_{i=1}^{n-h_1} \sum_{j=1}^{m-h_2} (X_{ij} - \bar{X})(X_{i+h_1, j+h_2} - \bar{X}).$$

The autocovariances are estimated for all lags up to an upper bound $\mathbf{b}^{(n,m)} = (b_1^{(n)}, b_2^{(m)})$, all other autocovariances are set to 0. In this paper, $b_i^{(k)} = \lfloor 0.9k^{(1/3)} \rfloor$ is used since it resembles the recommendations of Andrews (1991) for kernel density estimation, and it showed good results in preliminary studies.

Having obtained the estimated autocovariances, we can order the data matrix X into a vector $x = \text{vec}(X)$. Then, using all estimated $\hat{\gamma}(\mathbf{h})$, we construct the estimated autocovariance matrix $\hat{\Sigma}$ of the data vector x . To obtain the square root of the matrix $\hat{\Sigma}$, we perform a Cholesky decomposition, or the revised modified Cholesky decomposition (Schnabel and Eskow (1990)) if the estimated autocovariance matrix is not positive-semidefinite. We then invert this square root using the default R function `inv()`, that is based on the LAPACK routine DGESV (Anderson et al. (1999)). If the assumption of separability of the covariance function is justified, we can reduce the costs of decomposing and inverting $\hat{\Sigma}$ by estimating two smaller covariance matrices: one for the horizontal ($\hat{\Sigma}_1 \sim (m \times m)$) and one for the vertical ($\hat{\Sigma}_2 \sim (n \times n)$) direction. Then it holds $\hat{\Sigma} = \hat{\Sigma}_1 \otimes \hat{\Sigma}_2$. Accordingly, $\hat{\Sigma}_1$ and $\hat{\Sigma}_2$ can be estimated, decomposed, and inverted separately, reducing computation time from $O(n^3 m^3)$ to $O(n^3 + m^3)$. It follows that $\hat{\Sigma}^{-\frac{1}{2}} = \hat{\Sigma}_1^{-\frac{1}{2}} \otimes \hat{\Sigma}_2^{-\frac{1}{2}}$. The de-correlation process can then be performed as $y = \hat{\Sigma}^{-\frac{1}{2}}(x - \bar{x})$. Finally, we reorder y back into a matrix Y column-wise. Instead of the regular autocovariances, one could also use a difference-based approach (see e.g. Tecuapetla-Gómez and Munk (2017)). In the subsequent simulation study, we also investigated the behavior of the tests using such a difference-based estimator, but could not find any meaningful differences to the regular one. Alternatively, if a suitable model for the data is known, one could fit that model and apply tests to its residuals for further analysis.

5. Simulation study

In this section we analyze the finite sample behavior of the GMD and the VAR test under the hypothesis of a constant mean and under several alternatives. We do so using Monte Carlo simulations. The simulations are conducted using the software R (R Core Team (2024), version 4.4.3) along with the packages `SChangeBlock` (Görz (2025)), `robcp` (Görz and Dürre (2025)), and `ggplot2` (Wickham (2016)).

5.1. Setup

As a variance estimator for scaling the test statistic, we choose the ordinary sample variance

$$\hat{\sigma}^2 = \frac{1}{N-1} \sum_{i=1}^n \sum_{j=1}^m (X_{ij} - \bar{X})^2.$$

It is consistent and converges to the true variance σ^2 in $O\left(\frac{1}{\sqrt{N}}\right)$ under the hypothesis and appropriate assumptions for the noise, where N is the total number of observations. We choose the dimension of a random field to be $n \times n$ such that $n = m$ and $N = n^2$. To build the blocks, we choose $s_n = s_m = s$ around 0.6 such that for the block length $l_n = \lfloor n^s \rfloor$ and the number of blocks per dimension $b_n = \lfloor n/l_n \rfloor$ it holds $l_n \cdot b_n = n$. Preliminary studies indicated that both tests work best if there neither are blocks at the edges of the random field that are smaller than the majority of the blocks, nor if such blocks are left out completely. For generating the process variables $(Y_{i,j} : i, j \in \{1, \dots, n\})$ we consider three different distributions, namely the standard normal distribution $Y_{i,j} \sim \mathcal{N}(0, 1)$, the t -distribution

with 3 degrees of freedom $Y_{i,j} \sim t_3$, and the χ^2_2 distribution with 2 degrees of freedom, that equals an $\text{Exp}(1/2)$ distribution. Contrary to the requirements in Theorem 1, the t_3 distribution does not possess finite $(4+\varepsilon)$ -th absolute moments.

To incorporate dependency, we use a symmetric Spatial Moving Average model of order q (short: SMA(q)):

$$Y_{ij} = \sum_{k=-q}^q \sum_{l=-q}^q \theta_{kl} \varepsilon_{kl}.$$

The parameters (θ_{kl}) are either chosen as $\theta_{kl} = \rho^{|k-q-1|+|l-q-1|}$ for a pure SMA(q) model with a constant $\rho \in (-1, 1)$. This yields $M = q$ -dependent data. Alternatively, we choose

$$\theta_{ij} = \frac{\tilde{\theta}_{ij}}{\sqrt{\sum_{|k| \leq q_1} \sum_{|\ell| \leq q_2} \tilde{\theta}_{k\ell}^2}}$$

for $|i|, |j| \leq q$, with $\tilde{\theta}_{ij} = \varphi \sqrt{i^2 + j^2}$ as suggested by Steland (2025), since such a process with $q \geq 40$ approximates a spatial AR(1) process with parameter ρ . The distribution of the noise (ε_{kl}) is chosen to be standard normal. For the simulations, we consider an SMA(1) and a SAR(1) model, each with parameters $\rho \in \{0, 0.1, 0.2, 0.3\}$. In the case of $\rho = 0$, independent data are generated, but opposed to the study under independence, we investigate the behavior of the tests if de-correlation is unnecessarily applied.

We test the hypothesis of a constant μ in $X_{ij} = \mu(i/n, j/m) + Y_{ij}$, $1 \leq i, j \leq n$, against the alternative that μ changes across the field. For instance, μ could abruptly shift in some area or μ could steadily increase from one end of the field to the other. We will investigate the behavior of the tests on the following four different alternatives:

$$\begin{aligned} \mathbb{A}_1: \quad \mu(x, y) &= \frac{H}{\sqrt{nm}} \cdot \mathbb{1}_{\{1 \leq x \leq \frac{1}{n}\}} \mathbb{1}_{\{1 \leq y \leq \frac{1}{m}\}} \\ \mathbb{A}_2: \quad \mu(x, y) &= \frac{H}{\sqrt{nm}} \cdot \mathbb{1}_{\{1 \leq y \leq \frac{1}{2}\}} \\ \mathbb{A}_3: \quad \mu(x, y) &= \frac{H}{\sqrt{nm}} \cdot \frac{y-1}{m-1} \\ \mathbb{A}_4: \quad \mu(x, y) &= \frac{H}{\sqrt{nm}} \cdot \left(\mathbb{1}_{\{\frac{1}{4} \leq x \leq \frac{1}{2}\}} \mathbb{1}_{\{1 \leq y \leq \frac{1}{2}\}} + \mathbb{1}_{\{1 \leq x \leq \frac{1}{4}\}} \mathbb{1}_{\{\frac{1}{4} \leq y \leq \frac{1}{2}\}} \right) \end{aligned}$$

Figure 2 displays the alternatives presented here, along with markings on how the blocks are constructed. The

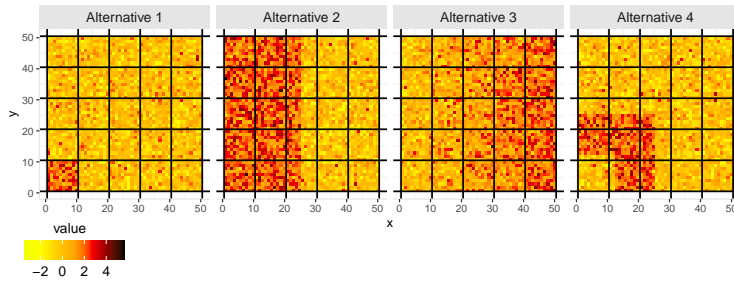


Figure 2: Examples of alternatives

shifts in \mathbb{A}_1 , \mathbb{A}_2 and \mathbb{A}_4 have a height of $\frac{H}{n}$, $H \in \{0, 10, 20, 50\}$, as we expect a shift in location to have a roughly quadratic impact. In \mathbb{A}_3 , the ascent is linear with a shift of 0 at x_{11}, \dots, x_{1n} up to a shift of $\frac{H}{n}$ at x_{n1}, \dots, x_{nn} . Under the hypothesis of no change, we set $\mu \equiv 0$. All results are obtained based on 1000 replications each at a significance level $\alpha = 0.05$.

5.2. Results under independence

Table 1 displays empirical sizes for $n \in \{10, 20, 50\}$ and all three innovation distributions under the null hypothesis, rounded to three digits. The size of the GMD test exceeds the significance level at $n = 10$ with values between 0.086

and 0.091. For a larger sample size, the test keeps the significance level. For 1000 repetitions, the standard deviation is about 0.0069, and only for the combinations GMD, $n = 10$ and Var, $\mathcal{N}(0, 1)$, $n = 50$, the empirical sizes lies outside of two standard deviations from 0.05. This problem for $n = 10$ does not occur with the Var test and we conclude that the GMD test needs a larger sample size, such as $n, m \geq 20$ to work properly under the hypothesis. All in all, even though the significance level is not seriously infringed, both tests show a slightly liberal behavior.

n	$\mathcal{N}(0, 1)$		t_3		χ^2_2	
	GMD	Var	GMD	Var	GMD	Var
10	0.091	0.046	0.086	0.047	0.089	0.050
20	0.058	0.056	0.048	0.049	0.048	0.053
50	0.053	0.064	0.054	0.051	0.052	0.058

Table 1: Empirical sizes of the GMD and the Var test under the hypothesis at nominal significance level $\alpha = 0.05$ for $n \in \{10, 20, 50\}$ and different innovation distributions, rounded to three digits.

The three plots in Figure 3 depict size-corrected power curves of both the GMD and the Var test for $n \in \{10, 20, 50\}$ and all three noise distributions for alternatives \mathbb{A}_1 to \mathbb{A}_4 . In case of alternative \mathbb{A}_1 , the Var test shows higher rejection

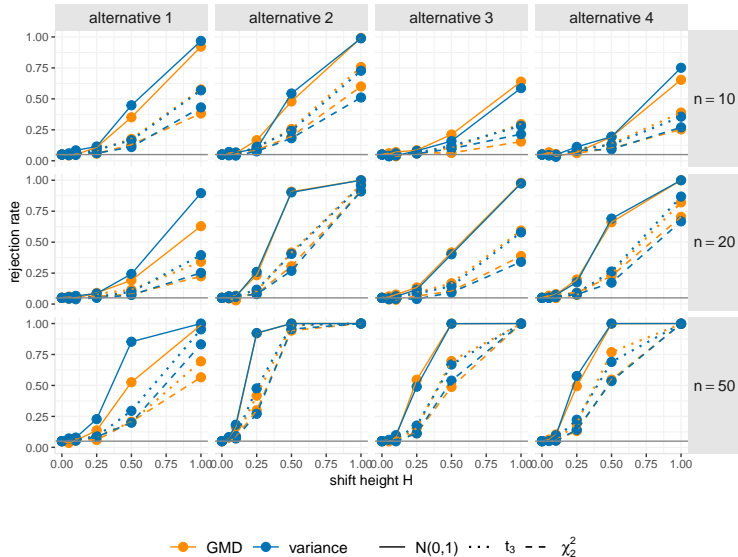


Figure 3: Size-corrected rejection rates of the GMD (orange) and the Var (blue) test at the nominal significance level $\alpha = 0.05$ as a function of location shift H , for $n = 10, 20, 50$, alternatives \mathbb{A}_1 to \mathbb{A}_4 and $\mathcal{N}(0, 1)$ (solid), t_3 (dotted), χ^2_2 (dashed) distributed innovations.

rates for all sample sizes and noise distributions considered here. This is probably due to the higher robustness of the mean difference as a measure of variability, compared to the ordinary variance. As a result, the GMD test ignores the single shifted block in this alternative more often. For $n = 10$ we need to consider that although the size-corrected power curves look similar, the Var test has an advantage over the GMD test as the latter struggles to keep the significance level for this sample size. As expected, both tests have the highest power under \mathbb{A}_2 where exactly half of the data is shifted. We conclude that both abrupt changes and trends can be detected quite reliably. Detailed values for shift height $H = 0.5$ can be found in the Appendix in Table B.1. Apart from these findings, we do not detect further relevant differences between the two tests. Even for t_3 -distributed noise, which does not possess $(4 + \varepsilon)$ -th moments as required by the Var test, this test still yields good results. Due to the slight advantages of the Var test, we will concentrate on this method in the following.

5.3. Results under dependence

Table 2 contains the empirical rejection rates of the Var test for SMA(1) and SAR(1) with different parameters ρ . Note that for $\rho = 0$, we are in the case of independent data, therefore there are no differences between SMA and SAR. We notice that especially for $\rho \in \{0.2, 0.3\}$ and a smaller n , the test has some problems in keeping the significance

	n	$\rho = 0$	$\rho = 0.1$	$\rho = 0.2$	$\rho = 0.3$
SMA(1)	10	0.052	0.052	0.043	0.037
	20	0.033	0.033	0.034	0.032
	50	0.044	0.044	0.040	0.036
SAR(1)	10	0.052	0.059	0.064	0.067
	20	0.033	0.042	0.060	0.115
	50	0.044	0.042	0.057	0.034

Table 2: Empirical sizes of the Var test at nominal significance level $\alpha = 0.05$ for $n \in \{10, 20, 50\}$ and both SMA(1) and SAR(1) random fields with parameter $\rho \in \{0, 0.1, 0.2, 0.3\}$ under the hypothesis, rounded to three digits.

level for SAR fields, with values between 0.060 and 0.115. In these cases, the dependence is rather strong and de-correlation alone probably does not suffice anymore or the autocovariances were underestimated. Apart from that, the level is kept very well and can even be seen as slightly conservative for some combinations.

Figures 4 and 5 display the size-corrected rejection rates of the Var test for SMA(1) and SAR(1) random fields. Here, we investigate location shifts up to a height of 4 opposed to 1 in the previous scenario. The first detail striking the eye is that all power curves display a drop for some shift height before regaining power for even higher shifts. This can be explained by the necessity of estimating the autocovariance. Due to the location shifts, the autocovariance is

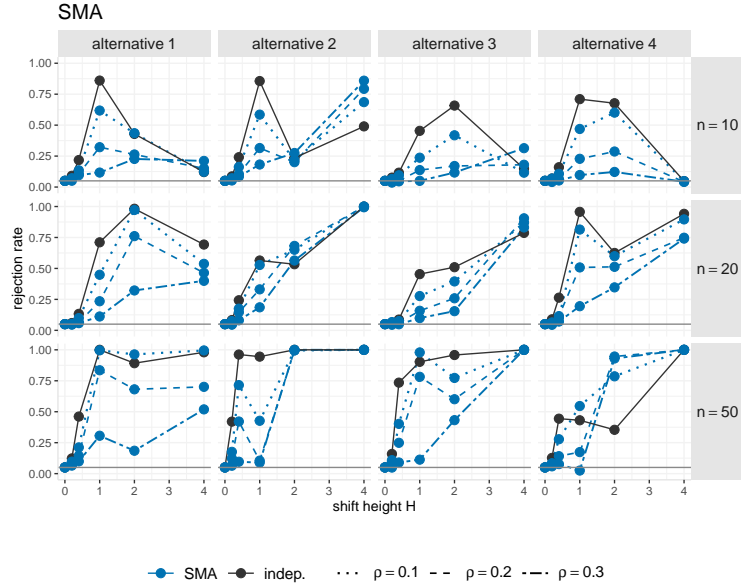


Figure 4: Size-corrected rejection rates of the Var test at the nominal significance level $\alpha = 0.05$ as a function of location shift H , for $n = 10, 20, 50$, alternatives \mathbb{A}_1 to \mathbb{A}_4 , for independent (black) and SMA(1) (blue) fields with parameter $\rho \in \{0.1, 0.2, 0.3\}$.

overestimated, which leads to a stronger de-correlation and then to a loss of power. For larger shifts, this overestimation can be compensated, and we see a convergence to 100% rejection rates for $n \geq 20$. For a simple alternative like \mathbb{A}_2 , the testing procedure also works well for $n = 10$. In Figure 4, we see that the power for SMA(1) fields rises faster than that for SAR(1) fields in Figure 5. However, since SMA(1) fields appear to be more prone to overestimation

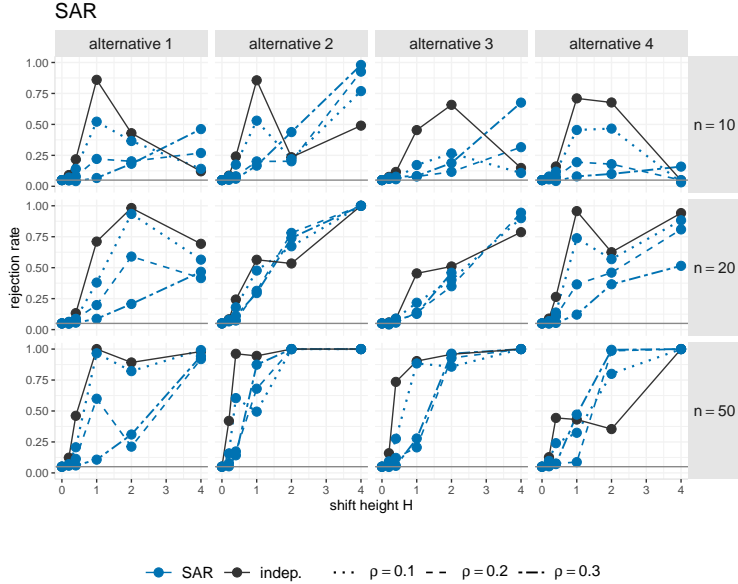


Figure 5: Size-corrected rejection rates of the Var test at the nominal significance level $\alpha = 0.05$ as a function of location shift H , for $n = 10, 20, 50$, alternatives \mathbb{A}_1 to \mathbb{A}_4 , for independent (black) and SAR(1) (blue) fields with parameter $\rho \in \{0.1, 0.2, 0.3\}$.

of autocovariances, they also experience a larger drop in power before regaining it. Detailed values for shift height $H = 2$ can be found in the Appendix in Table B.2. If the test was applied to independent residuals of a model fitted to the data, the results might improve, but having such good model is rare. As we see from the plots, good results can still be obtained without further knowledge about the dependency structure of the data. We also investigated how the power behaves when the GMD test is applied to the de-correlated data instead of the Var test, but no major differences between the two test could be detected, considering the known difficulties with alternative \mathbb{A}_1 .

6. Application to satellite images

The following example illustrates the application of the two tests to de-correlated satellite data obtained from the Landsat 8 satellite. This satellite is part of the NASA landsat project and collects data of the earth's land surface on 9 different spectral bands in the visible and short-wave infrared spectral regions (Knight and Kvaran (2014)). Such satellite imagery helps us to observe the earth's surface and recognize changes in time. The data can be accessed from <https://earthexplorer.usgs.gov/>. To be able to process the data in R, we used the packages `gdalcubes` (Appel and Pebesma (2019), Appel et al. (2021)), `magrittr` (Bache and Wickham (2022)), `xts` (Ryan and Ulrich (2024)), `magick` (Ooms (2024)) and `tidyverse` (Wickham et al. (2019)).

We used data from a small region of the Brazilian amazon rainforest, captured on August 12, 2014 and on July 19, 2017. The coordinates of the region are between -7355090 and -7351340 in latitude, and -1023760 and -1019440 in longitude in the EPSG:3857 format. Each pixel comprises a square of 30×30 meters. In total, we get two images with the size of 144×125 pixel each.

Our interest is to determine whether deforestation has taken place. To do so, we consider the Normalized Difference Vegetation Index (NDVI). This is a vegetation index measuring the greenness of biomass. It is calculated from the red (visible) and near-infrared spectral bands and takes values between -1 and 1. The greener the biomass, the higher the NDVI. Negative values do not usually occur on land (Myneni et al. (1995); Tucker (1979)).

Figure 6 illustrates the NDVI images captured on two different dates. On the left, the image predominantly displays green areas, with only one very small yellow dot on the right border. In contrast, the right image reveals large yellow-brownish patches that indicate parcels of land where trees have been cut down. The original images, sized at 144×125 pixels, are too large to be de-correlated effectively, even under the assumption of a separable

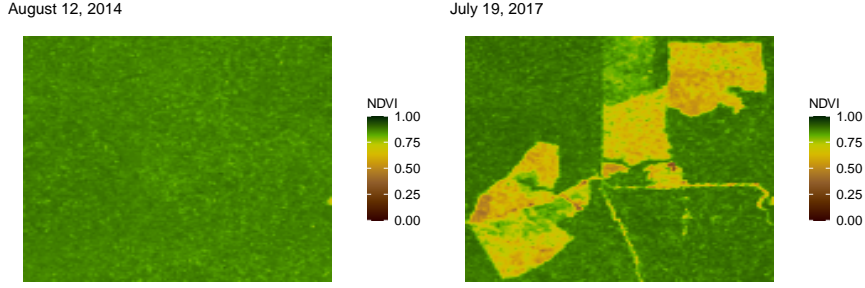


Figure 6: NDVI images of size 144×125 each (left: 2014, right: 2017)

covariance function. Doing so would require excessive time and computational resources. Additionally, the "green" in the 2014 image might still show some slight structure, with certain parts appearing darker than others. Therefore, we divide each image into 30 sub-images, where every sub-images measures 24×25 pixels. Figure 7 displays these split images from both 2014 and 2017. This segmentation simplifies the de-correlation process as we only need to

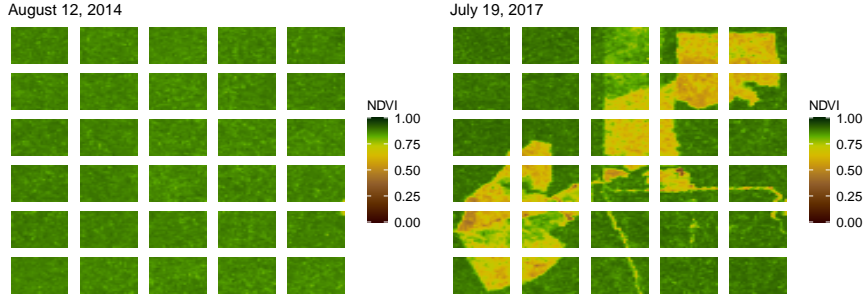


Figure 7: NDVI sub-images after splitting into 5×6 images of size 24×25 each (left: 2014, right: 2017)

invert 30 matrices of size 600×600 for each image. The plots in Figure 8 show the de-correlated data from both time points, where each sub-image has been de-correlated individually. In the left plot depicting the data from 2014, we observe only noise without any distinct structure. Conversely, in the right plot displaying the data from 2017, several

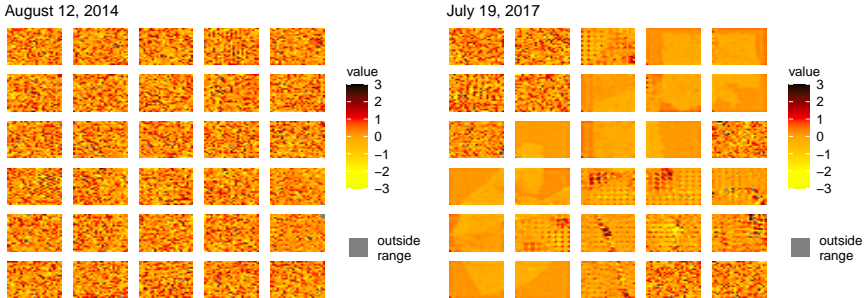


Figure 8: De-correlated sub-images (left: 2014, right: 2017)

deforested areas are clearly visible. Table 3 shows the test results of the Var test on the de-correlated sub-images for both dates. Values that are significant at a 5% level after Bonferroni-Holm correction are displayed in red. In the left table, there is only one significant p-value, corresponding to the sub-image at position (5, 5) containing part of the visible dot, while the test results are not significant for the other sub-images. As opposed to this, the right table displays 18 significant values. For all sub-images with a significant p-value, we can clearly see deforestation in

0.837	0.607	0.061	0.496	0.108	0.097	0.678	0.000	0.000	0.000
0.178	0.133	0.078	0.355	0.265	0.195	0.444	0.000	0.000	0.000
0.299	0.648	0.084	0.639	0.826	0.724	0.000	0.000	0.000	0.534
0.336	0.113	0.505	0.531	0.090	0.000	0.000	0.000	0.000	0.261
0.286	0.504	0.483	0.185	0.000	0.000	0.000	0.593	0.000	0.670
0.701	0.589	0.392	0.542	0.075	0.000	0.000	0.496	0.765	0.362

Table 3: p-values of the Var test on the de-correlated sub-images from August 12, 2014 (left) and Juli 19, 2017 (right), rounded to three digits. Values significant to a 5% level after Bonferroni-Holm correction are marked in red.

the original images (Figure 7). Only four images, namely at positions (6, 3), (5, 3), (4, 5) and (5, 5), show signs of deforestation caused by roads, but the test could not reject the hypothesis. This is expected as our test is by construction able to detect all change regions with positive Lebesgue measure consistently, but not lines. For all sub-images without deforestation, the test correctly did not reject the hypothesis.

7. Summary

We have introduced two tests for arbitrary changes in location for random fields, the GMD test extension of the method of Schmidt (2024) for two-dimensional data, and the Var test as an extension of the classical ANOVA. The tests assume independent observations and the existence of $2 + \varepsilon$ (GMD test) resp. $4 + \varepsilon$ (Var test) central moments. We have shown the convergence of the test statistic of the Var test to a normal distribution, and its consistency against all Lebesgue-measurable change regions. For the GMD test, both these properties can be deduced from the proofs in Schmidt (2024). In a simulation study, we have demonstrated that both tests can also successfully be applied to correlated data after de-correlation. In an application to satellite images, we showed that the Var test can reliably detect regions affected by deforestation.

Acknowledgments

This research was (partially) funded in the course of TRR 391 Spatio-temporal Statistics for the Transition of Energy and Transport (520388526) by the Deutsche Forschungsgemeinschaft (DFG, German Research Foundation). The authors gratefully acknowledge the computing time provided on the Linux HPC cluster at TU Dortmund University (LiDO3), partially funded in the course of the Large-Scale Equipment Initiative by the Deutsche Forschungsgemeinschaft (DFG, German Research Foundation) as project 271512359.

References

Amirkhani, F., Amiri, A., 2020. A novel framework for spatiotemporal monitoring and post-signal diagnosis of processes with image data. *Quality and Reliability Engineering International* 36, 705–735.

Anderson, E., Bai, Z., Bischof, C., Blackford, S., Demmel, J., Dongarra, J., Du Croz, J., Greenbaum, A., Hammarling, S., McKenney, A., Sorensen, D., 1999. LAPACK Users' Guide. Third ed., Society for Industrial and Applied Mathematics, Philadelphia, PA. URL: https://netlib.org/lapack/lug/lapack_lug.html.

Andrews, D.W., 1991. Heteroskedasticity and autocorrelation consistent covariance matrix estimation. *Econometrica: Journal of the Econometric Society* 59, 817–858.

Apostol, T.M., 1974. Mathematical Analysis. Second edition ed., Addison-Wesley.

Appel, M., Pebesma, E., 2019. On-demand processing of data cubes from satellite image collections with the gdal-cubes library. *Data* 4. URL: <https://www.mdpi.com/2306-5729/4/3/92>.

Appel, M., Pebesma, E., Mohr, M., 2021. Cloud-based processing of satellite image collections in r using stac, cogs, and on-demand data cubes. URL: <https://r-spatial.org/r/2021/04/23/cloud-based-cubes.html>. blog post on r-spatial.org.

Bache, S.M., Wickham, H., 2022. magrittr: A Forward-Pipe Operator for R. URL: <https://CRAN.R-project.org/package=magrittr>. r package version 2.0.3.

Billingsley, P., 2013. Convergence of probability measures. John Wiley & Sons.

Brillinger, D.R., 1962. A note on the rate of convergence of a mean. *Biometrika* 49, 574–576.

Bucchia, B., 2014. Testing for epidemic changes in the mean of a multiparameter stochastic process. *Journal of Statistical Planning and Inference* 150, 124–141.

Csörgő, M., Horváth, L., 1997. Limit theorems in change-point analysis. Wiley, Chichester.

Fuentes, M., 2005. A formal test for nonstationarity of spatial stochastic processes. *Journal of Multivariate Analysis* 96, 30–54.

Gromenko, O., Kokoszka, P., Reimherr, M., 2017. Detection of change in the spatiotemporal mean function. *Journal of the Royal Statistical Society Series B: Statistical Methodology* 79, 29–50.

Görz, S., 2025. SChangeBlock: Spatial structural change detection by an analysis of variability between blocks of observations. URL: <https://github.com/SGoerz/SChangeBlock>. r package version 0.0.1.

Görz, S., Dürre, A., 2025. robcp: Robust Change-Point Tests. URL: <https://cran.r-project.org/package=robcp>. r package version 0.3.8.

Jiang, B., Wang, C.C., Liu, H.C., 2005. Liquid crystal display surface uniformity defect inspection using analysis of variance and exponentially weighted moving average techniques. *International Journal of Production Research* 43, 67–80.

Kirch, C., Klein, P., Meyer, M., 2025. Scan statistics for the detection of anomalies in m-dependent random fields with applications to image data. *Journal of the American Statistical Association* , 1–20.

Knight, E.J., Kvaran, G., 2014. Landsat-8 operational land imager design, characterization and performance. *Remote sensing* 6, 10286–10305.

Mayrhofer, M., Radojičić, U., Filzmoser, P., 2025. Robust covariance estimation and explainable outlier detection for matrix-valued data. *Technometrics* , 1–15.

Myneni, R.B., Hall, F.G., Sellers, P.J., Marshak, A.L., 1995. The interpretation of spectral vegetation indexes. *IEEE Transactions on Geoscience and remote Sensing* 33, 481–486.

Okhrin, Y., Petruk, V., Schmid, W., 2025. Monitoring time dependent image processes for detecting shifts in pixel intensities. *Computational Statistics* , 1–32.

Okhrin, Y., Schmid, W., Semeniuk, I., 2020. New approaches for monitoring image data. *IEEE Transactions on Image Processing* 30, 921–933.

Ooms, J., 2024. magick: Advanced Graphics and Image-Processing in R. URL: <https://CRAN.R-project.org/package=magick>. r package version 2.8.4.

Otto, P., Schmid, W., 2016. Detection of spatial change points in the mean and covariances of multivariate simultaneous autoregressive models. *Biometrical Journal* 58, 1113–1137.

R Core Team, 2024. R: A Language and Environment for Statistical Computing. R Foundation for Statistical Computing. Vienna, Austria. URL: <https://www.R-project.org/>.

Robbins, M., Gallagher, C., Lund, R., Aue, A., 2011. Mean shift testing in correlated data. *Journal of Time Series Analysis* 32, 498–511.

Ryan, J.A., Ulrich, J.M., 2024. xts: eXtensible Time Series. URL: <https://CRAN.R-project.org/package=xts>. r package version 0.14.0.

Schmidt, S.K., 2024. Detecting changes in the trend function of heteroscedastic time series. *Bernoulli* 30, 2598–2622.

Schmidt, S.K., Wornowizki, M., Fried, R., Dehling, H., 2021. An asymptotic test for constancy of the variance under short-range dependence. *The Annals of Statistics* 49, 3460–3481.

Schnabel, R.B., Eskow, E., 1990. A new modified cholesky factorization. *SIAM Journal on Scientific and Statistical Computing* 11, 1136–1158.

Serfling, R.J., 1980. Approximation theorems of mathematical statistics. John Wiley & Sons.

Steland, A., 2025. Detection of suspicious areas in non-stationary gaussian fields and locally averaged non-gaussian linear fields. *Journal of Statistical Planning and Inference* 238, 106273.

Tecuapetla-Gómez, I., Munk, A., 2017. Autocovariance estimation in regression with a discontinuous signal and m-dependent errors: A difference-based approach. *Scandinavian Journal of Statistics* 44, 346–368.

Tucker, C.J., 1979. Red and photographic infrared linear combinations for monitoring vegetation. *Remote sensing of Environment* 8, 127–150.

Wickham, H., 2016. *ggplot2: Elegant Graphics for Data Analysis*. Springer-Verlag New York. URL: <https://ggplot2.tidyverse.org>.

Wickham, H., Averick, M., Bryan, J., Chang, W., McGowan, L.D., François, R., Grolemund, G., Hayes, A., Henry, L., Hester, J., Kuhn, M., Pedersen, T.L., Miller, E., Bache, S.M., Müller, K., Ooms, J., Robinson, D., Seidel, D.P., Spinu, V., Takahashi, K., Vaughan, D., Wilke, C., Woo, K., Yutani, H., 2019. Welcome to the tidyverse. *Journal of Open Source Software* 4, 1686. doi:10.21105/joss.01686.

Zhang, X., Zhu, Z., 2019. Spatial cusum for signal region detection. arXiv preprint arXiv:1904.03246 .

Appendix A. Detailed proofs

Proof of Proposition 2. Let $h, k \in \{1, \dots, b_n\} \times \{1, \dots, b_m\}$ be fixed. We notice that

$$(Y_{ij}^{(n,m)}) = (Y_{ij}^{(n,m)}; i, j \in \mathcal{I}_{hk}; n, m \in \mathbb{N})$$

is a double array. For every combination of $n, m \in \mathbb{N}$ the random variables $(Y_{ij}^{(n,m)})_{i,j}$ are independent. When defining $S_{hk}^{(n,m)} := \sum_{i,j \in \mathcal{I}_{hk}} Y_{ij}$, we can rewrite the statistic as

$$\sqrt{l_n l_m} \frac{\hat{Y}_{hk}^{(n,m)}}{\sigma} = \frac{S_{hk}^{(n,m)}}{\sqrt{l_n l_m \sigma^2}}$$

and it holds

$$E(S_{hk}^{(n,m)}) = E\left(\sum_{i,j \in \mathcal{I}_{hk}} Y_{ij}\right) = \text{Var}(S_{hk}^{(n,m)}) = \text{Var}\left(\sum_{i,j \in \mathcal{I}_{hk}} Y_{ij}\right) = l_n l_m \sigma^2.$$

For the proposition to hold, we need to verify Lyapunov's condition. Denote with M_k the k -th central moment of Y_{ij} , then we get

$$\frac{1}{\text{Var}(S_{hk}^{(n,m)})^{1+\frac{\delta}{2}}} \sum_{i,j \in \mathcal{I}_{hk}} E(|Y_{ij}|^{2+\delta}) = \frac{1}{(l_n l_m \sigma^2)^{1+\frac{\delta}{2}}} \sum_{i,j \in \mathcal{I}_{hk}} M_{2+\delta} = O\left(\frac{1}{(l_n l_m)^{\frac{\delta}{2}}}\right).$$

□

Appendix B. Tables and figures

	$\mathcal{N}(0, 1)$		t_3		χ^2_2	
	GMD	Var	GMD	Var	GMD	Var
$n = 10$						
\mathbb{A}_1	0.482	0.409	0.253	0.172	0.216	0.117
\mathbb{A}_2	0.618	0.538	0.335	0.229	0.249	0.163
\mathbb{A}_3	0.251	0.175	0.136	0.098	0.135	0.089
\mathbb{A}_4	0.378	0.288	0.227	0.138	0.150	0.093
$n = 20$						
\mathbb{A}_1	0.250	0.257	0.103	0.114	0.098	0.105
\mathbb{A}_2	0.938	0.925	0.400	0.439	0.300	0.307
\mathbb{A}_3	0.413	0.389	0.124	0.148	0.123	0.124
\mathbb{A}_4	0.688	0.687	0.253	0.261	0.169	0.210
$n = 50$						
\mathbb{A}_1	0.580	0.846	0.228	0.318	0.166	0.238
\mathbb{A}_2	1.000	1.000	0.988	0.987	0.949	0.948
\mathbb{A}_3	0.999	1.000	0.687	0.718	0.548	0.535
\mathbb{A}_4	1.000	1.000	0.712	0.746	0.565	0.578

Table B.1: Simulated rejection rates of the GMD and the Var test at the nominal significance level $\alpha = 0.05$ for a location shift $H = 0.5$, $n = 10, 20, 50$, and different innovation distributions under the alternatives \mathbb{A}_1 to \mathbb{A}_4 , rounded to three digits.

	SMA(1)			SAR(1)			
	$\rho = 0.1$	$\rho = 0.2$	$\rho = 0.3$	$\rho = 0.1$	$\rho = 0.2$	$\rho = 0.3$	$\rho = 0$
\mathbb{A}_1	0.437	0.261	0.166	0.383	0.215	0.205	0.455
\mathbb{A}_2	0.270	0.195	0.230	0.210	0.228	0.446	0.246
\mathbb{A}_4	0.592	0.329	0.108	0.473	0.220	0.137	0.661
\mathbb{A}_3	0.407	0.151	0.112	0.318	0.125	0.204	0.628
\mathbb{A}_1	0.952	0.737	0.265	0.935	0.598	0.323	0.987
\mathbb{A}_2	0.612	0.651	0.563	0.653	0.809	0.875	0.432
\mathbb{A}_4	0.564	0.462	0.316	0.585	0.493	0.532	0.625
\mathbb{A}_3	0.353	0.206	0.132	0.426	0.394	0.540	0.499
\mathbb{A}_1	0.960	0.699	0.159	0.810	0.247	0.328	0.880
\mathbb{A}_2	0.998	0.997	0.998	1.000	1.000	1.000	0.999
\mathbb{A}_4	0.780	0.969	0.920	0.790	0.988	0.992	0.345
\mathbb{A}_3	0.747	0.583	0.421	0.848	0.915	0.961	0.970

Table B.2: Simulated rejection rates of the Var test at the nominal significance level $\alpha = 0.05$ for a location shift $H = 2$, $n = 10, 20, 50$, SMA(1) and SAR(1) models with parameters $\rho \in \{0.1, 0.2, 0.3\}$ and independent data ($\rho = 0$) under the alternatives \mathbb{A}_1 to \mathbb{A}_4 , rounded to three digits.